

When Casimir meets Kibble–Zurek

G Vacanti¹, S Pugnetti², N Didier², M Paternostro³, G M Palma⁴,
R Fazio^{1,2} and V Vedral^{1,5,6}

¹ Center for Quantum Technologies, National University of Singapore, 1 Science Drive 2, Singapore

² NEST, Scuola Normale Superiore and Istituto Nanoscienze-CNR, I-56126 Pisa, Italy

³ School of Mathematics and Physics, Queen's University, Belfast BT7 1NN, UK

⁴ NEST Istituto Nanoscienze-CNR and Dipartimento di Fisica, Università degli Studi di Palermo, via Archirafi 36, I-90123 Palermo, Italy

⁵ Clarendon Laboratory, University of Oxford, Parks Road, Oxford OX1 3PU, UK

⁶ Department of Physics, National University of Singapore, 3 Science Drive 4, Singapore

E-mail: giova.physics@gmail.com

Received 30 April 2012

Accepted for publication 27 June 2012

Published 30 November 2012

Online at stacks.iop.org/PhysScr/T151/014071

Abstract

Verification of the dynamical Casimir effect (DCE) in optical systems is still elusive due to the very demanding requirements for its experimental implementation. This typically requires very fast changes in the boundary conditions of the problem. We show that an ensemble of two-level atoms collectively coupled to the electromagnetic field of a cavity, driven at low frequencies and close to a quantum phase transition, stimulates the production of photons from the vacuum. This paves the way for an effective simulation of the DCE through a mechanism that has recently found experimental demonstration. The spectral properties of the emitted radiation reflect the critical nature of the system and allow us to link the detection of DCE to the Kibble–Zurek mechanism for the production of defects when crossing a continuous phase transition.

PACS number: 42.50.Pq

(Some figures may appear in colour only in the online journal)

1. Introduction

When N two-level atoms interact collectively with a single mode of the electromagnetic field inside a cavity, thus realizing the so-called Dicke model [1], there is a critical value of the atom–photon coupling g_c at which the system undergoes a quantum phase transition, generally referred to as the *super-radiant transition*. Below the critical coupling the atoms are in their ground level and no photons are present. In contrast, above g_c there is a spontaneous symmetry breaking and the photon field gets populated through a mechanism producing a displaced coherent state [2]. The experimental demonstration of the super-radiant transition in the Dicke model has remained outstanding until recently, when a key result was achieved in a setup involving intra-cavity Bose–Einstein condensates [3]. A super-radiant transition has been enforced by exploiting the spatial self-organization of the atoms in an intra-cavity condensate coupled to the cavity field and subjected to an optical-lattice potential.

Close to a quantum phase transition there is an intimate relation between equilibrium and dynamical properties. The critical slowing down, characteristic of continuous phase transitions, suggests that the response to a time-periodic external drive may be highly non-trivial. In the case of the super-radiant transition there are two additional fundamental reasons to look for the response of the system to an external ac drive: the detection of the dynamical Casimir effect (DCE) [4, 5] and the investigation of the Kibble–Zurek mechanism (KZM) [6, 7]. Notwithstanding some interesting proposals [8–11] having the potential to ease the requirements for its observability, an experimental demonstration of DCE is still elusive in the optical domain, due to the prohibitively large frequencies at which the system's parameter should be modulated to produce a measurable flux of photons. Here, we prove that, at the super-radiant transition, a DCE-like mechanism arises from the use of a time-dependent driving and results in a flux of photons generated from the vacuum fluctuations. Recently, DCE was observed in an experiment

performed using microwaves [12]. Our proposal pursues a different direction: we observe that, on approaching the Dicke super-radiant phase transition, the frequencies at which the DCE-like effect becomes observable are lowered, thus narrowing the gap separating the experimental state-of-the-art from the observation of the effect.

Moreover, we unveil an intriguing connection between the occurrence of DCE through the mechanism we propose and the KZM. The latter predicts the formation of defects in a quantum many-body system dragged through a critical point [13–15] and is due to the inability of the system to remain in its ground state. The production of defects occurs regardless of how slowly the dragging is performed and the mechanism has been shown to be related to adiabatic quantum computation [16] and quantum annealing [17]. We are thus able to bridge two fundamental phenomena in out-of-equilibrium quantum systems with the goal of simplifying their observation. The recent demonstration of the Dicke super-radiant transition [3], which is the building block of our proposal, marks a promising starting point towards an experimental investigation along the lines of our work.

The paper is organized as follows. In section 2, we will consider the case in which all the dissipative processes can be neglected and the system undergoes a unitary evolution. In section 3, we will extend our analysis to the case when the cavity experiences photon losses and we will show that a constant flux of photons is present in the output field of the cavity when the system's parameters are modulated in time. Finally, in section 4 we will link the generation of photons arising from the DCE to the KZM, presenting qualitative and quantitative evidence of the connection between the two phenomena.

2. The system's Hamiltonian and unitary evolution

We study a system consisting of N two-level atoms placed inside a cavity in which the splitting between the ground and excited states of each atom can be modulated in time. In this section, we first review some interesting properties of the system's Hamiltonian in the absence of modulation [18] and then address the case of a time-dependent Hamiltonian, solving the unitary dynamics of the system.

Let us consider a system formed by N two-level atoms interacting with the fundamental mode of the field inside a cavity. We assume that the splitting between the ground and the excited level of each atom can be externally modulated in time. The fundamental mode of the cavity is described using the annihilation and creation operators \hat{a} and \hat{a}^\dagger and each two-level atom is treated as a pseudo-spin with angular momentum components $\{\hat{\sigma}_+^i, \hat{\sigma}_-^i, \hat{\sigma}_z^i\}$. Assuming that the atoms interact with the field in a collective way, the whole atomic cloud is described by the total angular momentum \hat{J} with components $\hat{J}_\pm = \sum_i \hat{\sigma}_\pm^i$ and $\hat{J}_z = \sum_i \hat{\sigma}_z^i$. Within this notation and setting $\hbar = 1$, the Hamiltonian of the system in the absence of modulation and in the dipole approximation reads as

$$H_0 = \omega_a \hat{a}^\dagger \hat{a} + \omega_b \hat{J}_z + \frac{g}{\sqrt{2j}} (\hat{a}^\dagger + \hat{a})(\hat{J}_+ + \hat{J}_-), \quad (1)$$

where ω_b is the static atomic splitting, which is assumed to be the same for every atom, ω_a is the fundamental frequency of

the cavity and g is the atom–field coupling constant. Here j is the so-called ‘cooperation number’ in the Dicke theory and is an eigenvalue of \hat{J}^2 .

When the number of atoms N becomes large, the Holstein–Primakoff representation of angular momentum can be used to formally assimilate the atomic cloud to an harmonic oscillator [19]. Using this representation, the components of the angular momentum \hat{J} can be written in terms of bosonic annihilation and creation operators \hat{b} , \hat{b}^\dagger . Since the number of atoms is large, a good approximation for the Holstein–Primakoff equations is given by $\hat{J}_+ \approx \sqrt{2j} \hat{b}^\dagger$, $\hat{J}_- \approx \sqrt{2j} \hat{b}$ and $\hat{J}_z = (\hat{b}^\dagger \hat{b} - j)$. Substituting these expressions in equation (1) and neglecting the overall shifting term, the Hamiltonian becomes

$$H_0 = \sum_{k=a,b} \omega_k \hat{k}^\dagger \hat{k} + g (\hat{a}^\dagger + \hat{a})(\hat{b}^\dagger + \hat{b}) \quad (2)$$

with $k = \{a, b\}$.

The Hamiltonian in equation (2) describes two harmonic oscillators coupled via an xx interaction with coupling constant g and can be exactly diagonalized. Considering the position and momentum operators for the two modes, $x_k = (1/\sqrt{2\omega_k})(\hat{k}^\dagger + \hat{k})$ and $y_k = i\sqrt{(\omega_k/2)}(\hat{k}^\dagger - \hat{k})$, the diagonal form is obtained by rotating the coordinate system following the transformations $x_a = q_1 \cos \gamma + q_2 \sin \gamma$ and $x_b = -q_1 \sin \gamma + q_2 \cos \gamma$, where the angle γ is given by $\tan 2\gamma = (4g\sqrt{\omega_a\omega_b})/(\omega_b^2 - \omega_a^2)$. The rotated Hamiltonian (up to an overall shifting) reads as

$$H_0 = \frac{1}{2} \sum_{k=1,2} (\epsilon_k^2 \hat{q}_k^2 + \hat{p}_k^2), \quad (3)$$

where

$$\begin{aligned} \epsilon_1^2 &= \frac{1}{2} \left(\omega_a^2 + \omega_b^2 - \sqrt{(\omega_b^2 - \omega_a^2)^2 + 16g^2\omega_a\omega_b} \right), \\ \epsilon_2^2 &= \frac{1}{2} \left(\omega_a^2 + \omega_b^2 + \sqrt{(\omega_b^2 - \omega_a^2)^2 + 16g^2\omega_a\omega_b} \right). \end{aligned} \quad (4)$$

Equation (3) describes two uncoupled harmonic oscillators with frequencies ϵ_1 and ϵ_2 .

It can be noted from equation (4) that the value of ϵ_1 becomes imaginary when g exceeds the critical value $g_c = \sqrt{\omega_a\omega_b}/2$. That means that the system undergoes different behaviors depending on being in the ‘normal phase’ ($g < g_c$) or in the so-called ‘super-radiant phase’ ($g > g_c$), as explained in [18]. Indeed, the existence of this critical value is crucial for the argument we put forth. Since at this stage we are interested only in the normal phase regime, we will not go into the details of the phase transition process. Nevertheless, it is important to point out that the model described above is valid only for $g < g_c$ and that the critical nature of the system plays an important role.

We are now ready to address the case when the atomic splitting is sinusoidally modulated with frequency η and amplitude λ . This is in some sense a generalization of the scheme proposed in [10, 11], where a system consisting of a single two-level atom placed inside a cavity is studied. Let us consider the Hamiltonian given in equation (2) and let us assume that the atomic frequency is no longer ω_b but

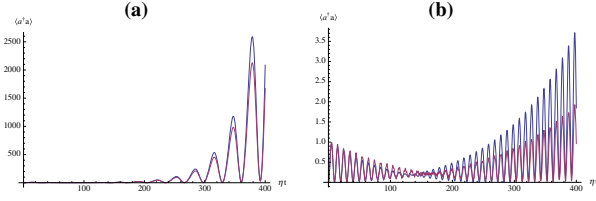


Figure 1. Mean number of photons inside a non-leaking cavity against time calculated using the Lewis–Riesenfeld method in the one-mode approximation (blue line) and solving the Heisenberg equations of motions for exact two-mode Hamiltonian (red line). The parameters are $\omega_a = \omega_b = 1$, $\eta = 2\epsilon_1$, $\lambda = 0.01$. The values of g are: (a) $g = 0.99g_c = 0.495$ and (b) $g = 0.9g_c = 0.45$.

a time-dependent function of the form $\Omega(t) = \omega_b + \lambda \sin \eta t$ instead. Substituting this expression into equation (2), the time-dependent Hamiltonian of the system becomes

$$H = \omega_a a^\dagger a + \Omega(t) b^\dagger b + g(a^\dagger + a)(b^\dagger + b). \quad (5)$$

The diagonalized Hamiltonian has the same form as the one given in equation (3), with time-dependent frequencies $\epsilon_k(t)$ which are obtained simply by substituting ω_b with $\Omega(t)$ in equation (4).

The unitary dynamics can be solved using two different methods. In both cases, we assume that the system is initialized in its ground state, i.e. with all the atoms in the lower energy level and the field in the vacuum state at $t = 0$. The first method consists of solving the Heisenberg equations of motion for the field operators a and a^\dagger and for the atomic cloud bosonic operators b and b^\dagger . The Heisenberg equations are given by $\dot{k} = -i[k, H]$ with $k = a, b$. The equations can be recast into an equation for the covariance matrix, which is solved numerically. Alternatively, the problem can be treated in the Schrodinger picture using the Lewis–Riesenfeld method [20, 21]. This method gives us a strategy for solving any time-dependent problem using the so-called dynamical invariants, and it is particularly useful in the case of quadratic Hamiltonians.

In this second case, we will make use of the diagonal form of the Hamiltonian in order to make some approximations. In the limit in which the modulation frequency η and the time-dependent frequencies $\epsilon_k(t)$ satisfy the conditions

$$\epsilon_2(t) \gg \eta, \quad \epsilon_2(t) \gg \epsilon_1(t), \quad (6)$$

the non-critical mode \hat{q}_2 will not contribute to the photon production. In the adiabatic approximation we can get rid of the second mode and describe the system as a single harmonic oscillator with a time-dependent frequency whose Hamiltonian is given by $H \approx (1/2)[\epsilon_1^2(t)\hat{q}^2 + \hat{p}^2]$. Comparing the results obtained in the two cases, we can test the validity of the one-mode approximation.

The quantity of interest in the DCE context is the mean number of photons $\langle a^\dagger a \rangle$ generated inside the cavity, which is calculated using the Lewis–Riesenfeld method in the single-mode approximation and using the Heisenberg equations for the exact two-mode Hamiltonian. We find that a modulation at frequency $\eta = 2\epsilon_1$ results in the generation of photons from vacuum inside the cavity. Moreover, as shown in figure 1, the number of photons generated increases when

the coupling constant g approaches its critical value g_c . The two results are very similar when the coupling constant is close to its critical value, e.g. $g = 0.99g_c$ (see figure 1(a)) as expected. With the decreasing of g the discrepancy between the two quantities increases (see figure 1(b)). This is due to the fact that the conditions in equation (6) are not fulfilled anymore when g is far away from the critical value g_c and the single-mode approximation is not valid any longer. This behavior is conditioned to the choice of the system's parameters. Indeed, g_c is now a time-dependent quantity and the system would go through a phase transition if $g_c < g$ at some time t , in which case the model used would fail and the results would no longer make sense. It is thus important to choose the system's parameters in such a way that the condition $g_c > g$ holds for all t . In analogy with the usual DCE and with the single-atom schemes proposed in [10, 11], the photons are created in pairs. On the other hand, while in these schemes the modulation frequency is required to be of the order of the photonic frequency, in our proposal η can be, in principle, as small as we want, due to the fact that $\epsilon_1 \rightarrow 0$ at the phase transition.

The model treated here resembles the many-body Landau–Zener problem studied in [22, 23] with the crucial difference of the inclusion of the counter-rotating terms in our analysis, which lead to *both* the super-radiant transition and the production of photons. It is also worth mentioning that in [24] a model similar to ours but based on a semi-classical approach has been addressed to relate DCE-like effects to Dicke super-radiance. In this work we perform a full quantum treatment of both the atom–light interaction and the effects on the photon statistics induced by the driving of the atomic subsystem. Moreover, as discussed in section 4, we will unveil a connection between the DCE-like effects and the KZ mechanism.

3. Dissipative dynamics: the Langevin equations approach

In the previous section, we have studied the case of a cavity with perfect mirrors and have shown how it is possible to generate photons by modulating the parameters of the system. In this section, we consider a leaking cavity in which the internal mode experiences photons' losses due to the coupling with the environment. Since we are neglecting atomic decays, the equation of motion for the bosonic operator b describing the atomic cloud is still the Heisenberg equation of motion $\dot{b} = -i[b, H]$. On the other hand, the cavity mode operator a is subjected to dissipative processes, and its open dynamics can be obtained by solving the Langevin equations of the system and making use of the input–output formalism for optical cavities [25].

To derive the Langevin equation describing the evolution of the system in the non-rotating frame, we start by assuming a cavity–bath interaction in the form of $V = i \int_0^\infty dv k_v (\alpha_v a^\dagger - \alpha_v^\dagger a)$. For a generic quadratic two-mode Hamiltonian, the equations of motion can be written in a compact matrix notation. Taking into account that mode b does not experience any dissipation, we define the bosonic operators vector as $u(t) = (a(t), b(t), a^\dagger(t), b^\dagger(t))^T$ and the Langevin forces vector as $F(t) = (f(t), 0, f^\dagger(t), 0)^T$. Within this notation,

the equations for the two modes in the domain of time can be rewritten in the form

$$\dot{u}(t) = -iM(t)u(t) - \int dt' \Gamma(t-t')u(t') + F(t), \quad (7)$$

where $M(t)$ is a time-dependent 4×4 matrix taking into account the unitary evolution and $\Gamma(t-t')$ is the 4×4 matrix of the damping kernels given by $\Gamma(t-t') = \text{diag}[\gamma(t-t'), 0, \gamma(t-t'), 0]$. It is worth mentioning that, when $M(t)$ is a periodic function of t with period T , it can be expanded as a Fourier series which, in general, is given by $M(t) = M(t+T) = \sum_m M_m e^{i\frac{2\pi}{T}mt}$.

Solving equation (7) might be a very hard task due to the presence of a non-trivial convolution integral. The problem can be avoided by moving in the domain of frequencies. Since the matrix $M(t)$ explicitly depends on time, by moving to the frequencies domain we need to consider all the sideband contributions coming from the Fourier decomposition. Defining $\tilde{u}(\omega) = (\tilde{a}(\omega), \tilde{b}(\omega), \tilde{a}^\dagger(-\omega), \tilde{b}^\dagger(-\omega))^T$ and $\tilde{F}(\omega) = (\tilde{f}(\omega), 0, \tilde{f}^\dagger(-\omega), 0)^T$ as the Fourier transform of the vectors $u(t)$ and $F(t)$ introduced above, the Langevin equations in the domain of frequencies read as [27]

$$i\mathcal{M}(\omega) \begin{pmatrix} \tilde{u}(\omega - m\eta) \\ \vdots \\ \tilde{u}(\omega + m\eta) \end{pmatrix} = \begin{pmatrix} \tilde{F}(\omega - m\eta) \\ \vdots \\ \tilde{F}(\omega + m\eta) \end{pmatrix}, \quad (8)$$

where the matrix $\mathcal{M}(\omega)$ is given by

$$\mathcal{M}(\omega) = \begin{pmatrix} B_{-m} & M_1 & \dots & M_{2m} \\ M_{-1} & B_{-(m-1)} & & \vdots \\ \vdots & & & M_1 \\ M_{-2m} & \dots & M_{-1} & B_m \end{pmatrix} \quad (9)$$

and where $B_j = M_0 - (\omega + j\eta) - i\tilde{\Gamma}(\omega + j\eta)$. Here $\tilde{\Gamma}(\omega) = \text{diag}[\tilde{\gamma}(\omega), 0, \tilde{\gamma}(-\omega), 0]$ is the Fourier transform of the damping memory kernel and $\eta = 2\pi/T$. The Langevin force operators $\tilde{f}(\omega)$ in the domain of frequencies are linked to the input operators of the cavity by $\tilde{f}(\omega) = 2\pi k_\omega \rho(\omega) \alpha_\omega^{\text{in}}$, where $\rho(\omega)$ represents the photonic density of states of the bath [26]. On the other hand, following [26] again, the decay rates can be written in the domain of frequencies as $\tilde{\gamma}(\omega) = \text{Re}[\tilde{\gamma}(\omega)] + i\text{Im}[\tilde{\gamma}(\omega)]$. While the imaginary part of $\tilde{\gamma}(\omega)$ is just a fixed Lamb shift, the real part $\text{Re}[\tilde{\gamma}(\omega)] = \pi |k_\omega|^2 \rho(\omega)$ is responsible for the frequency-depending damping of the cavity mode. When the counterrotating terms are taken into account it becomes crucial to consider that the density of photonic state in the bath $\rho(\omega)$ is zero for negative frequencies. It follows immediately that $\tilde{\gamma}(\omega) = 0$ and $\tilde{f}(\omega) = 0$ for $\omega < 0$. In the following, we will also suppose that the damping rate assumes the same value for every positive frequency. This is equivalent to assuming that $k_\omega = k \forall \omega$ and $\rho(\omega) = 1$ for $\omega > 0$. Within this assumption, we define $\gamma_0 \equiv \pi |k|^2$ and we can write $\text{Re}[\tilde{\gamma}(\omega)] = \gamma_0$ for $\omega > 0$ and $\text{Re}[\tilde{\gamma}(\omega)] = 0$ for $\omega < 0$.

We start our analysis by calculating the mean number of photons inside the cavity at the stationary state $\langle a^\dagger a \rangle$, which is given by $\langle a^\dagger a \rangle = \lim_{t \rightarrow \infty} \langle a^\dagger(t) a(t) \rangle$.

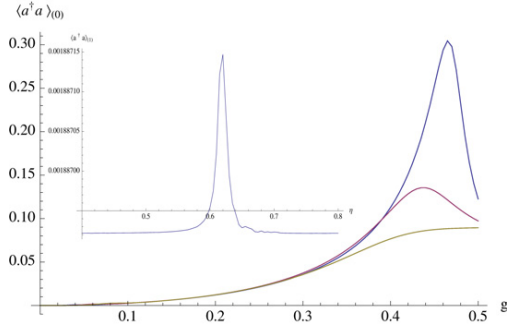


Figure 2. (Main panel) The mean number of photons inside a leaking cavity against the interaction constant g in the case of no-modulation for $\gamma_0 = 0.1$ (blue line), $\gamma_0 = 0.2$ (red line) and $\gamma_0 = 0.3$ (yellow line). (Inner panel) The mean number of photons inside a leaking cavity against the modulation frequency η for $\lambda = 0.00005$ and $\gamma_0 = 0.005$ and $g = 0.45 = 0.9g_c$.

After Fourier transformation, the limit gives $\langle a^\dagger a \rangle = (1/2\pi)^2 \int_{-\infty}^{\infty} d\omega \langle \tilde{a}^\dagger(\omega) \tilde{a}(\omega) \rangle$. For the Hamiltonian considered here, the matrix $M(t)$ includes a sinusoidal modulation with period $T = (2\pi)/\eta$. Its Fourier expansion is thus given by $M(t) = M_0 + M_1(e^{i\eta t} - e^{-i\eta t})$. So the Fourier expansion of $M(t)$ counts just the three components M_0 , M_1 and $M_{-1} = -M_1$. The solution of equation (8) can be found simply by inverting the matrix $i\mathcal{M}$. Calling $\mathcal{G}(\omega) = [i\mathcal{M}(\omega)]^{-1}$ and solving for $\tilde{a}(\omega)$, the mean number of photons is given by

$$\langle a^\dagger a \rangle_{(m)} = \frac{\gamma_0}{\pi} \sum_{j=-m}^m \int_{j\eta}^{\infty} d\omega |\mathcal{G}_{4m+1, 4(m+j)+3}(-\omega)|^2, \quad (10)$$

where the index (m) indicates the number of sidebands taken into account and $\mathcal{G}_{i,j}(\omega)$ are the matrix elements of $\mathcal{G}(\omega)$. To obtain equation (10), we have assumed that the input field is in the vacuum state, so the operators $\alpha_\omega^{\text{in}}$ fulfill the condition $\langle \alpha_\omega^{\text{in}} \alpha_{\omega'}^{\text{in}} \rangle = \delta(\omega - \omega')$ and we have made use of the fact that the state's density function is given by $\rho(\omega) = 1$ for $\omega > 0$ and $\rho(\omega) = 0$ for $\omega < 0$.

Let us now consider the explicit calculation of the mean number of photons inside the cavity in two simple cases. The first example is the case when $m = 0$, i.e. no time-dependent modulation is applied to the system (see [26] for more details). In this case equation (10) simply reduces to

$$\langle a^\dagger a \rangle_{(0)} = \frac{\gamma_0}{\pi} \int_0^{\infty} d\omega |\mathcal{G}_{1,3}(-\omega)|^2. \quad (11)$$

The behavior of the number of photons $\langle a^\dagger a \rangle_{(0)}$ against the interaction constant g for various values of the decay rate γ is shown in the main panel of figure 2. It is important to point out that the non-vanishing mean number of photons is related to the presence of virtual photons which are trapped inside the cavity and cannot be observed. Indeed, due to the energy conservation law, it is impossible for the photons to leave the cavity and be detected when the Hamiltonian of the system is time-independent and the input field is in the vacuum state. We will see shortly that the number of photons leaking out of the cavity is identically zero when no-modulation is applied. Another simple example is given by considering a

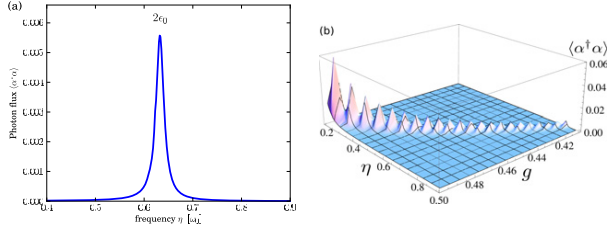


Figure 3. Radiation flux outside the cavity. (a) Flux of photons outside the cavity against η for $g/\omega_a = 0.9$, $g_c/\omega_a = 0.45$, $\gamma/\omega_a = 0.005$ and $\lambda/\omega_a = 0.005$. For these parameters, $\epsilon_0/\omega_a \approx 0.315$. (b) Flux of photons outside the cavity against η and g for $\omega_b/\omega_a = 1$, $\gamma/\omega_a = 0.005$ and $\lambda/\omega_a = 0.005$.

weak modulation, in which case we can assume that only the first two sidebands give a significant contribution (i.e. $m = 1$). The number of photons is then given by

$$\langle a^\dagger a \rangle_{(1)} = \frac{\gamma_0}{\pi} \int_{-\eta}^{\infty} d\omega |\mathcal{G}_{5,3}(-\omega)|^2 + \frac{\gamma}{\pi} \int_0^{\infty} d\omega |\mathcal{G}_{5,7}(-\omega)|^2 + \frac{\gamma}{\pi} \int_{\eta}^{\infty} d\omega |\mathcal{G}_{5,11}(-\omega)|^2. \quad (12)$$

The quantity $\langle a^\dagger a \rangle_{(1)}$ is shown in the inner panel of figure 2 as a function of the modulating frequency η . The plot shows a sharp resonance peak at $\eta = 2\epsilon_1$, as expected from the previous analysis in the unitary regime, with the difference that in a leaking cavity the system reaches a stationary state when the photons' creation rate equals the cavity damping rate.

We now pass to the explicit calculation of the flux of photons leaking out of the cavity for the two cases treated above. To obtain the output operator of the cavity $\alpha_\omega^{\text{out}}$, we substitute the solution for the internal operator $\tilde{a}(\omega)$ into the input–output relation for an optical cavity [25]. The photonic flux outside the cavity is given by $\langle \alpha^\dagger \alpha \rangle = \int_0^{\infty} d\omega \langle \alpha_\omega^{\text{out} \dagger} \alpha_\omega^{\text{out}} \rangle$. This expression is very similar to the one giving the number of photons inside the cavity, with the crucial difference that only positive frequencies of the bath are included in the integration. Assuming again that $\langle \alpha_\omega^{\text{in}} \alpha_{\omega'}^{\text{in} \dagger} \rangle = \delta(\omega - \omega')$, $\rho(\omega) = 0$ for $\omega < 0$ and $\rho(\omega) = \gamma_0$ for $\omega > 0$, $\langle \alpha^\dagger \alpha \rangle$ reads as

$$\langle \alpha^\dagger \alpha \rangle_{(m)} = 4\gamma_0^2 \sum_{j=0}^m \int_0^{\eta} d\omega |\mathcal{G}_{4m+1,4(m-j)+3}(\omega)|^2. \quad (13)$$

Note that, having the matrix elements of \mathcal{G} the dimension of time, the quantity $\langle \alpha^\dagger \alpha \rangle$ has the correct dimension of $1/t$ for a flux of photons.

It can be seen immediately from equation (13) that, as expected and according to energy conservation law, no photons' flux outside the cavity is observed when $m = 0$, i.e. when no modulation is applied and the Hamiltonian is time-independent. In contrast, any time-dependent modulation generates a constant flux of photons. For $m = 1$, equation (13) counts just one term given by

$$\langle \alpha^\dagger \alpha \rangle_{(1)} = 2\gamma_0^2 \int_0^{\eta} d\omega |\mathcal{G}_{5,3}(\omega)|^2. \quad (14)$$

The flux of photons $\langle \alpha^\dagger \alpha \rangle_{(1)}$ is plotted against the modulation frequency η and the coupling constant g in figure 3. In

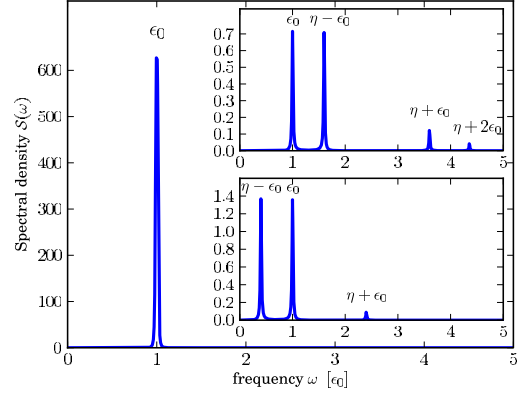


Figure 4. Spectral density of the output photons. Taking $\omega_a = \omega_b = 1$, $\lambda = 0.005$, $\gamma = 0.005$, $g = 0.9$ and $g_c = 0.45$, we find that $\epsilon_0 = 0.315$. We have taken $\eta/2\epsilon_0 = 1$ (corresponding to resonance conditions; the main panel), $\eta/2\epsilon_0 = 0.7$ (upper inset) and $\eta/2\epsilon_0 = 1.3$ (lower inset).

panel (a), a resonance peak is clearly visible at $\eta \approx 0.63$ when $g = 0.9g_c = 0.45$. For this value of g , the value of the smallest eigenvalue ϵ_1 given in equation (4) is $\epsilon_1 \approx 0.315$. So, as expected, the resonance occurs at $\eta \approx 2\epsilon_1$. This profile is the same as the one relative to the photons' flux inside the cavity shown in figure 2. In panel (b), the flux of photons is plotted against g and η . It can be seen that the resonance occurs at $\eta \approx 2\epsilon_1$ regardless of the value of ϵ_1 . Moreover, the photons' flux at the resonance increases when g approaches its critical value g_c . It is thus evident that bringing the system close to its critical point presents the double advantage of reducing the frequency at which the DCE is observable and increasing the number of photons generated in the process.

In the last part of this section, we analyze the spectral density $\mathcal{S}(\omega)$ of the output flux of photons, which is linked to the spectral density inside the cavity $\mathcal{P}(\omega)$ via the input–output relations. To find $\mathcal{P}(\omega)$, we consider the autocorrelation function for the number of photons inside the cavity at the stationary state (i.e. for $t \rightarrow \infty$), which is defined as $F(\tau) = \lim_{t \rightarrow \infty} \langle a^\dagger(t + \tau)a(t) \rangle$ [28]. Substituting the Fourier transform of $a(t)$ and $a^\dagger(t)$, the equation above becomes $F(\tau) = \int_{-\infty}^{\infty} d\omega \langle a^\dagger(\omega)a(\omega) \rangle e^{-i\omega\tau}$. Being the spectral density $\mathcal{P}(\omega)$ defined as the Fourier transform of the autocorrelation function, it follows that $\mathcal{P}(\omega) = \langle a^\dagger(\omega)a(\omega) \rangle$. Considering the input–output relations and that $\pi|k_\omega|^2 = \gamma_0$, the spectral density of the output flux of photons can be immediately written as $\mathcal{S}(\omega) = (\gamma_0/\pi)\mathcal{P}(\omega)$. In the case of a weak modulation where only the first two sidebands are taken into account and $m = 1$, $\mathcal{S}(\omega)$ is non-vanishing only for $0 < \omega < \eta$ and can be written as

$$\mathcal{S}(\omega) = 4\gamma_0^2 |\mathcal{G}_{5,3}(-\omega + \eta)|^2. \quad (15)$$

The spectral density outside the cavity $\mathcal{S}(\omega)$ for a weak modulation is plotted in figure 4 for various values of the modulation frequency η . When $\eta = \eta_{\text{res}} = 2\epsilon_1$, the spectrum reveals a single sharp peak at $\omega \approx \epsilon_1$ (main panel). In the non-resonant regime, the emission at $\omega \approx \epsilon_1$ is drastically reduced and other sideband emission lines appear (inner panels).

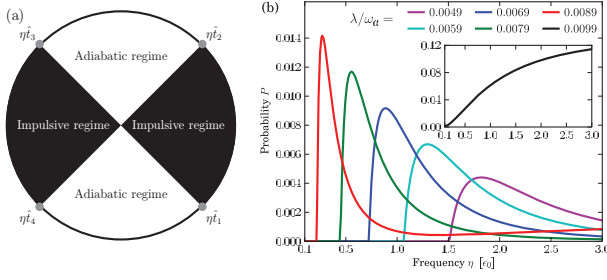


Figure 5. (a) Schematic representation of the four freeze-out points in the trigonometric circle. (b) Probability of leaving the ground state against η/ϵ_0 for $g = 0.49/\omega_a$ and various values of λ .

4. Connection with the Kibble–Zurek mechanism

Finally, we address the crucial connection between our DCE-like mechanism and the Kibble–Zurek one [6, 7]. In this section, we consider only the single-mode approximation, and thus we drop the index and set $\epsilon_1(t) \equiv \epsilon(t)$ to simplify the notation. On approaching the critical point of the model in equation (1), regardless of the value of η , there will always be a regime where the perturbation is non-adiabatic and photons are produced. A first estimate of the unavoidable departure from adiabaticity, with a consequent photon flux, is obtained by calculating the probability of the system to go into an excited state. For simplicity, we consider one period in the absence of damping. The probability of leaving the ground state at the final time t_f (t_i being the initial time) is

$$P = 1 - |\langle \Psi(t_f) | \varphi_0(t_f) \rangle|^2 \quad (16)$$

with $|\varphi_n(t)\rangle$ being the instantaneous eigenstates of the harmonic oscillator and $|\Psi(t_f)\rangle$ the final state of the system. The KZM relies on the assumption that the state of a system brought close enough to the critical point *freezes* when the system is not able to adiabatically follow the changes in the control parameter. For the driving here at hand, the freeze-out times is found by solving the equation

$$\mathcal{T}(t)/\dot{\mathcal{T}}(t) = \tau(t), \quad (17)$$

where $\mathcal{T}(t) = g_c(t)/g - 1$ plays the role of the relative temperature of the system and $\tau = \tau_0/\epsilon(t)$ is its relaxation time ($\tau_0 = 1/\omega$).⁷ For a sinusoidal modulation of $\mathcal{T}(t)$ and if the oscillating terms brings the system sufficiently close to the critical point, one finds four solutions, each embodying a freeze-out time. Figure 5(a) shows their representations in the unit circle. As the system is initialized in its ground state, i.e. $|\Psi(t_i)\rangle = |\varphi_0(t_i)\rangle$, the adiabatic condition $\mathcal{T}(t)/\dot{\mathcal{T}}(t) > \tau$ is satisfied until $t = \hat{t}_1$, where \hat{t}_1 is the freeze-out time at which the system enters the so-called impulsive regime. During this period, the state of the system is frozen until $t = \hat{t}_2$, when the adiabatic condition is fulfilled again and the state of the system becomes $|\Psi(\hat{t}_2)\rangle = |\varphi_0(\hat{t}_2)\rangle = \sum_n c_{n,0}(\hat{t}_2, \hat{t}_1) |\varphi_n(\hat{t}_2)\rangle$, where $c_{n,m}(t, t') = \langle \varphi_n(t) | \varphi_m(t') \rangle$. The same argument applies to the second part of the cycle, where the system evolves adiabatically for $t \in [\hat{t}_2, \hat{t}_3]$ and is frozen for $t \in [\hat{t}_3, \hat{t}_4]$.

⁷ Note that $\mathcal{T}(t)$ is defined as $\mathcal{T}(t) = 1 - g(t)/g_c$ if the time-dependent parameter is g instead of ω .

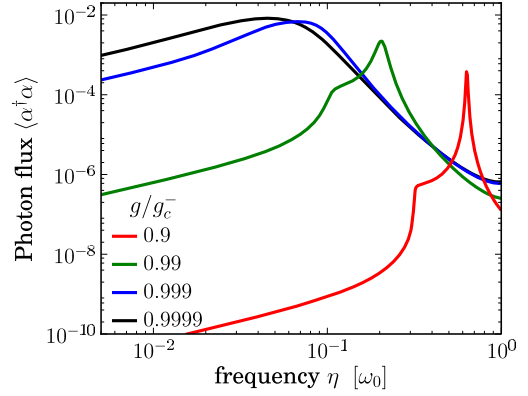


Figure 6. Output photon flux as a function of η for different values of g . The transition between the adiabatic and non-adiabatic regimes (sharp step) is located at the minimum of the gap and is shifted to lower frequency when the coupling gets closer to the critical coupling. At the critical point the dynamics is purely non-adiabatic.

The state at \hat{t}_4 is then

$$|\Psi(\hat{t}_4)\rangle = \sum_{k,n} c_{k,n}(\hat{t}_4, \hat{t}_3) c_{n,0}(\hat{t}_2, \hat{t}_1) e^{-i\theta_n} |\varphi_k(\hat{t}_4)\rangle, \quad (18)$$

where $\theta_n = \int_{\hat{t}_2}^{\hat{t}_3} dt E_n(t)$. Finally, the last part of the evolution ($t \in [\hat{t}_4, t_f]$) will not affect the probability P , which is thus given by

$$P = 1 - |\langle \Psi(\hat{t}_4) | \varphi_0(\hat{t}_4) \rangle|^2. \quad (19)$$

The behavior of the probability P against η is shown in figure 5(b) for different values of λ . Clearly, the closer the system to the quantum phase transition, the more it is susceptible to a low-frequency driving. A more detailed analysis requires the study of the transient dynamics. The scheme of figure 5(a) is still valid, the probability of excitations being calculated by composing four different dissipative maps in the same spirit of [29]. We expect only quantitative changes.

To corroborate the connection between DCE and KZM, we have further analyzed the photon production in the adiabatic and non-adiabatic regimes (cf figure 6). For $\eta > \epsilon_{\min}$ (ϵ_{\min} being the minimum value of $\epsilon(t)$ over a cycle), the dynamics is non-adiabatic and photons can be created. Close to criticality, the minimum of the gap vanishes, the system is always in the non-adiabatic regime and the photon flux increases linearly with η until the maximum value at resonance is reached. Far from the transition, the photon production decreases from the resonance with a Lorentzian behavior: when $\eta < \epsilon_{\min}$, the photon flux is sharply reduced and a linear behavior is recovered but with a much smaller value. This abrupt transition between the adiabatic and non-adiabatic regimes demonstrates that the breakdown of adiabaticity due to critical slowing down is at the origin of photon creation in the DCE, a situation totally analogous to what is described by the KZM.

5. Conclusions

We have proposed a scheme to realize the DCE by exploiting the dragging of a driven quantum Dicke model across its

critical point. By modeling the atom–field interaction as a linear coupling between two harmonic oscillators, we have made use of the peculiar features of a critical system close to a quantum phase transition to simplify the observation of DCE in the optical frequencies range. In particular, the reduction of the energy gap between the ground and the first excited state has been exploited in order to bring the modulation frequency at which the DCE is observable to the level of experimental feasibility. Moreover, by investigating the transition between the adiabatic and the non-adiabatic regime, we have been able to link the photon production arising from the DCE to another fundamental phenomenon in condensed matter systems, the KZM. Indeed, the connection between the DCE and the KZM, which is supported by qualitative and quantitative evidence in this work, emphasizes how both phenomena can be seen as a consequence of the inability of the system to adiabatically follow the parameters' changes.

Some comments are due regarding the observation of the photons' flux outside the cavity. Due to the small frequency of the photons generated when g approaches the critical value (the emission frequency is at $\omega \approx \epsilon_1$), the thermal noise in the output signal may be significant and the detection process may become a very demanding task. This problem can be avoided by considering a cavity in which the two mirrors are both semi-transparent and photons are allowed to come in and leak out of the cavity from both sides. Being the thermal baths in the two output fields completely uncorrelated, the noise signal can be virtually eliminated by measuring the correlations between the two output modes. Indeed, the study of such correlations can be regarded as a more general subject for further investigations.

We would like to emphasize the novelty and generality of our proposal. Differently from previous works, we address the problems involved in the experimental observation of DCE in the optical regime by exploiting the peculiarities of a critical system, using a full quantum approach and including dissipative processes in our model. Moreover, to the best of our knowledge, no connections have previously been established between the fundamental phenomena such as quantum phase transitions, DCE and KZM. Such a connection represents a crucial result of this work. Although we have explicitly considered a system formed by atoms trapped inside a cavity where the atomic energy splitting is modulated in time, our scheme can be applied to any system in which the Dicke model can be implemented and some parameter can be modulated in time. The last remark suggests a prompt realization of our proposal in the light of the recent

experimental achievement of the Dicke phase transition [3] in intra-cavity condensates coupled with the cavity field.

Acknowledgments

We acknowledge financial support from the National Research Foundation and the Ministry of Education of Singapore, the EU FP7 Programme under grant agreement numbers 234970-NANOCTM and 248629-SOLID, the UK EPSRC (EP/G004759/1) and EUROTCH. VV is a fellow of Wolfson College, Oxford.

References

- [1] Dicke R H 1954 *Phys. Rev.* **93** 99
- [2] Barnett S M and Radmore P M 2003 *Methods in Theoretical Quantum Optics* (Oxford: Oxford University Press)
- [3] Baumann K *et al* 2010 *Nature* **464** 1301
- [4] Yablonovitch E 1989 *Phys. Rev. Lett.* **62** 1742
- [5] Schwinger J 1992 *Proc. Natl Acad. Sci. USA* **89** 4091
- [6] Kibble T W B 1976 *J. Phys. A: Math. Gen.* **9** 1387
- [7] Zurek W H 1985 *Nature* **317** 505
- [8] Dodonov V V 2010 *Phys. Scr.* **82** 038105
- [9] Johansson J R, Johansson G, Wilson C M and Nori F 2009 *Phys. Rev. Lett.* **103** 147003
- [10] Dodonov A V *et al* 2008 arXiv:0806.4035v3
- [11] De Liberato S, Gerace D, Carusotto I and Ciuti C 2009 *Phys. Rev. A* **80** 053810
- [12] Wilson C M, Johansson G, Pourkabirian A, Simoen M, Johansson J R, Duty T, Nori F and Delsing P 2011 *Nature* **479** 376
- [13] Dziarmaga J 2010 *Adv. Phys.* **59** 1063
- [14] Zurek W H, Dorner U and Zoller P 2005 *Phys. Rev. Lett.* **95** 105701
- [15] Polkovnikov A 2005 *Phys. Rev. B* **72** 161201
- [16] Farhi E *et al* 2001 *Science* **292** 472
- [17] Santoro G E *et al* 2002 *Science* **295** 2427
- [18] Emary C and Brandes T 2003 *Phys. Rev. E* **67** 066203
- [19] Holstein T and Primakoff H 1940 *Phys. Rev.* **58** 1098
- [20] Lewis H R and Riesenfeld W B 1968 *J. Math. Phys.* **10** 1458
- [21] Bastidas V M *et al* 2009 arXiv:0910.1600v1
- [22] Altland A, Gurarie V, Kriecherbauer T and Polkovnikov A 2009 *Phys. Rev. A* **79** 042703
- [23] Altland A and Gurarie V 2008 *Phys. Rev. Lett.* **100** 063602
- [24] Kirilyuk I L 2002 *Opt. Spectrosc.* **92** 719
- [25] Walls D F and Milburn G J 2008 *Quantum Opt.* (Heidelberg: Springer)
- [26] Ciuti C and Carusotto I 2006 *Phys. Rev. A* **74** 033811
- [27] Mari A and Eisert J 2009 *Phys. Rev. Lett.* **103** 213603
- [28] Carmichael H J 2002 *Statistical Methods in Quantum Optics I* 2nd edn (Berlin: Springer)
- [29] Shytov A V, Ivanov D A and Feigel'man M V 2003 *Eur. Phys. J. B* **36** 263